Published in final edited form as:
J Immunol. 2014 April 1; 192(7): 3390–3398. doi:10.4049/jimmunol.1302525.

The RhoA GEF, LARG, mediates ICAM-1-dependent mechanotransduction in endothelial cells to stimulate transendothelial migration

Elizabeth C. Lessey-Morillon[1], **Lukas D. Osborne**[2], **Elizabeth Monaghan-Benson**[1], **Christophe Guilluy**[1], **E. Timothy O'Brien**[2], **Richard Superfine**[2], and **Keith Burridge**[1,3,4,*]

[1]Department of Cell Biology and Physiology, University of North Carolina, Chapel Hill, NC, 27599

[2]Department of Physics and Astronomy, University of North Carolina, Chapel Hill, North Carolina 27599

[3]Lineberger Comprehensive Cancer Center, University of North Carolina, Chapel Hill, North Carolina, 27599

[4]McAllister Heart Institute, University of North Carolina, Chapel Hill, North Carolina, 27599

Abstract

RhoA-mediated cytoskeletal rearrangements in endothelial cells (ECs) play an active role in leukocyte transendothelial cell migration (TEM), a normal physiological process in which leukocytes cross the endothelium to enter the underlying tissue. While much has been learned about RhoA signaling pathways downstream from ICAM-1 in ECs, little is known about the consequences of the tractional forces that leukocytes generate on ECs as they migrate over the surface before TEM. We have found that after applying mechanical forces to ICAM-1 clusters, there is an increase in cellular stiffening and enhanced RhoA signaling compared to ICAM-1 clustering alone. We have identified that the RhoA GEF LARG/ARHGEF12 acts downstream of clustered ICAM-1 to increase RhoA activity and that this pathway is further enhanced by mechanical force on ICAM-1. Depletion of LARG decreases leukocyte crawling and inhibits TEM. This is the first report of endothelial LARG regulating leukocyte behavior and EC stiffening in response to tractional forces generated by leukocytes.

Introduction

Leukocyte extravasation is a tightly controlled process that involves signaling in both the leukocyte and endothelial cell (EC). Neutrophils are early responders to sites of infection. Pro-inflammatory signals prompt them to exit post-capillary venules and infiltrate tissues to ingest microbes or foreign bodies, destroying them with proteolytic enzymes and/or the release of reactive oxygen species. In response to inflammatory signals, several adhesion molecules become expressed or increased on the EC surface including Inter-cellular adhesion molecule-1 (ICAM-1). Leukocyte transendothelial migration (TEM) starts with

*Address correspondence to Keith Burridge at CB#7295 UNC-CH, Chapel Hill, NC 27599, tel (919) 966-5783, fax (919) 966-3015, keith_burridge@med.unc.edu.

leukocyte rolling, mediated by leukocyte binding to selectins on the surface of ECs (1). β2 integrins on the leukocyte then bind to ICAM-1 (2–10). The strong adhesion resulting from ICAM-1 engagement and clustering allows leukocytes to spread and crawl on the surface of the endothelium. Finally, leukocytes cross the EC monolayer, either passing through the junctions or through the ECs themselves (9, 11, 12) to enter the underlying tissue. Without ICAM-1, leukocyte spreading, crawling and TEM are impaired (13, 14).

Engagement and clustering of ICAM-1 by leukocytes induces multiple signaling pathways within ECs (15) that promote passage of the leukocytes across the endothelium. After ICAM-1 clustering, F-actin and actin binding proteins associate with the clustered complex to assist in the cytoskeletal changes that occur during leukocyte adhesion and TEM (16–20). One of the pathways responsible for these changes involves the GTPase RhoA, which was shown to be activated following ICAM-1 engagement and clustering (5, 16). Inhibiting RhoA signaling in ECs reduces leukocyte adhesion, spreading, and migration (3, 4, 13, 21). RhoA is also activated by various agents, such as thrombin, that increase the permeability of EC junctions (22–24). In part, this is due to RhoA-stimulated actomyosin contraction that exerts tension on the junctions, however, there is additional evidence that the adhesive strength of the junctions is weakened by signaling downstream of active RhoA (25). Clustering of ICAM-1 also elevates tyrosine phosphorylation of multiple proteins and several studies have identified Src family kinases (SFKs) as being responsible and being activated downstream of ICAM-1 (19, 26–28). However, the relationship between SFK activity and Rho protein activation downstream from ICAM-1 has not been explored.

Cell migration requires the cell to exert tractional forces on the underlying substratum. The amount of traction force generated by migrating leukocytes has been estimated to be between 5 and 50 pN (29–31). It is unclear if EC signaling is altered in response to the tractional force applied by leukocytes to adhesion molecules expressed on the EC luminal surface. At the outset of this work, we were interested in determining whether the tractional forces exerted on ICAM-1 as leukocytes migrate affect RhoA signaling, and secondly, we were interested in identifying the guanine nucleotide exchange factor(s) (GEF) that activate RhoA downstream of ICAM-1. Here we identify LARG, also known as ARHGEF12, as the critical RhoA GEF activating RhoA downstream of ICAM-1, show that it is activated by SFK-dependent tyrosine phosphorylation, and demonstrate that applying mechanical force on ICAM-1 clusters equivalent to the forces generated by migrating neutrophils enhances this signaling pathway. We provide evidence that this activation of RhoA not only promotes neutrophil TEM but stiffens the endothelial surface thereby enhancing the migration of neutrophils over it.

Methods and materials

Reagents and antibodies

RhoA mAb and ICAM-1 mAb (western blotting) were purchased from Santa Cruz Biotechnology (Santa Cruz, CA). The mAb against MHC class I (HLA-A, -B, and -C) was purchased from BD Biosciences (Franklin Lakes, NJ). The pAb for LARG (for immunoprecipitation) was purchased from Abcam (Cambridge, MA). Phosphotyrosine mAb, clone 4G10, Y-27632, SU6656, and blebbistatin were purchased from Millipore

(Billerica, MA). pAb for p115, and phosphorylated myosin light chain (pMLC) (Thr18/Ser19) were purchased from Cell Signaling (Danvers, MA). pAb for LARG, and PDZ-RhoGEF were made against the c-terminal tail of the proteins (Pocono Rabbit Farm and Laboratory, Canadensis, PA). Recombinant TNF and stromal cell–derived factor-1 (CXCL12) was purchased from R&D Systems (Minneapolis, MN). αICAM-1 R6.5.D6 hybridoma was purchased from ATCC (Manassas, VA). mAb for tubulin, mAb for myosin light chain (MLC), and Cytochalasin D, were purchased from Sigma-Aldrich (St. Louis, MO). pAb for GEFH1was purchased from Bethyl (Montgomery, TX). mAb myc was purchased from Invitrogen (Grand Island, NY). Bovine Collagen Solution was purchased from Advanced BioMatrix (San Diego, CA). Fibronectin was isolated from human plasma as previously described (32). pAb p190RhoGEF (Rgnef) was a generous gift for Dr. David D. Schlaepfer (University of California San Diego).

Cell cultures and treatments

Neonatal human dermal blood microvascular ECs (HMVEC), pooled HUVEC, growth medium and supplements were purchased from Lonza (Walkersville, MD). ECs were cultured at 37°C and 5% CO_2. For all experiments, unless otherwise noted, HMVEC were grown on 10 μg/ml collagen until confluent for at least 24 h. For all biochemical experiments at least 10^4 mAb-coated beads were added per cm^2. For all magnetic tweezer experiments at least 10^3 beads were added per cm^2. Static force was applied by placing a ceramic magnet above the tissue culture dish for the specified length of time. Primary human neutrophils were isolated from donor blood drawn by BD Vacutainer ® CPT Cell Preparation Tubes (BD Biosciences) following the manufacture's protocol. Briefly, whole blood was spun for 15 min at 15,000 g. The granulocyte and red blood cell fractions were recovered and the RBCs lysed. The remaining neutrophils were re-suspended in complete EC medium containing 1% Human serum albumin and 1 mM HEPES. Institutional Review Board for University of North Carolina at Chapel Hill has approved all human subject protocols.

mAb-coated beads and force with the permanent magnet

αICAM-1 R6.5.D6 hybridomas were grown in Cell mAb Serum Free Media (BD Biosciences) in CELLine CL-1000 Flasks (BD Biosciences) and the Ig was purified from the hybridoma culture supernatant using a Protein AG UltraLink Resin (Thermo Fisher Scientific, Waltham, MA). Purified mAb was dialyzed in 0.1 M borate buffer, pH 9.5. Tosyl-activated Dynabeads M-450 Beads (Invitrogen, Carlsbad, CA) were prepared following the manufacturer's protocol. Briefly, beads were washed twice with 0.1 M borate buffer pH 9.5 and incubated with 1 μg/ml mAb per 10^6 beads in 0.1 M borate buffer pH 9.5 at 37°C. After 30 min fatty acid-free BSA was added for a final concentration of 0.01% and rotation continued overnight. For all biochemical experiments, a continuous force (~10 pN) was applied to mAb-coated beads using a permanent ceramic magnetic (K&J Magnetics, Jamison, PA) 1 cm above and parallel to the monolayer of ECs in the tissue culture dish.

Magnetic tweezer force assay

mAb-coated beads were added to ECs for approximately 10–20 min and bead tracking was initiated. Pulses of force (~160 pN) were applied on the beads using the UNC three-

dimensional force microscope. The magnetic tweezers were positioned ~25 microns above the monolayer (so as to avoid scraping the underlying monolayer of cells). Force was applied to individual beads at an acute angle. Cells were imaged using an 40x objective (Olympus UplanLN 40x/.75) on an Olympus IX81®-ZDC2 inverted microscope (Olympus) equipped with a high-speed Rolera EM-C2 camera (QImaging) to record bead movement using MetaMorph software at 30 frames per second. Bead movements above 70 nm were tracked by Video Spot Tracker (Center for Computer Integrated Systems for Microscopy and manipulation, http://http://cismm.cs.unc.edu). Before experiments began, the magnetic tweezer system was calibrated by applying a force ramp to magnetic beads in a Newtonian fluid of a known viscosity. By recording bead trajectories and computing bead velocities, Stokes law, $F = 6\pi a\eta v$, was used to determine the force, where a is the bead radius, η is the fluid viscosity, and v is the bead velocity. Knowledge of the bead displacement r(t) and the applied force F(t) allowed for computing the compliance signature, $J(t) = 6\pi ar(t)/F(t)$, which was then fit to a modified Kelvin-Voigt mechanical circuit model for viscoelastic liquids. The spring constant was reported as the local stiffness in pascals (Pa).

Preparation of recombinant proteins

pGEX GST-PBD and pGEX GST-RhoA^{G17A} fusion proteins were prepared from lysates from Bl21 *Escherichia coli* cells induced with 100 μM IPTG for 16 h at RT. For GST-RBD, bacterial cells were lysed in 20 mM Tris pH 7.8, 1% Triton 100, 10 mM $MgCl_2$ 1 mM DTT, 1mM PMSF, and 10 μg/ml aprotinin and leupeptin. For GST-RhoA^{G17A} bacterial cells were lysed in 20 mM HEPES pH 7.8, 150 mM NaCl, 10 mM $MgCl_2$, 1mM PMSF, and 10 μg/ml aprotinin and leupeptin. The recombinant proteins were isolated from the bacterial lysates by incubating with glutathione-Sepharose 4B beads (GE Healthcare) at 4°C for 4 h. The beads were sedimented and washed 3 times in 20 mM HEPES, pH 7.5; 150 mM NaCl mM DTT.

GST-RBD and GST-RhoA^{G17A} Pull-down Assay

RhoA activation assays were preformed as described (33). HUVECs were lysed in 300 μL of 10 mM $MgCl_2$, 500 mM NaCl, 50 mM Tris, pH 7.8, 1% Triton X-100, 0.1% SDS, 0.5% deoxycholate, 1mM PMSF, and 10 μg/ml aprotinin and leupeptin, cleared at 14,000g at 4°C for 3 min and incubated with at least 20 μg of GST-RBD for 20 min at 4°C. Beads were then washed 3x in 50 mM Tris, pH 7.4, 10 mM $MgCl_2$, 150 mM NaCl, 1% Triton X-100, 1mM PMSF, and 10 μg/ml aprotinin and leupeptin. Active GEFs were assayed by binding to GST-RhoA^{G17A} as described (34). In short it was performed as the RhoA activation assays with the following changes. HUVECs were lysed in 150 mM NaCl, 20 mM HEPES, pH 7.6, 10 mM $MgCl_2$, 1% Triton X-100 1mM PMSF, and 10 μg/ml aprotinin and leupeptin, and incubated with GST-RhoA^{G17A} beads for 60 min at 4°C and washed in the same lysis buffer. Samples were then analyzed by western blotting.

Western Blotting

Samples were run on SDS-PAGE gels and transferred to polyvinylidene fluoride membranes (Millipore). Membranes were blocked and incubated with the specified primary antibodies followed by species-specific secondary antibodies conjugated with horseradish peroxidase. Blots were developed with a chemiluminescent HRP substrate, and visualized on x-ray film.

For quantification, blots were scanned and the intensity values determined using Image J software (NIH) and protein levels were normalized to control protein levels. All quantification graphs include ≥3 independent experiments. Error bars represent SEM.

Phase contrast microscopy

HUVECs were grown collagen-coated coverslips for at least 72 h before imaging. HUVECs were treated with 5 ng/ml TNF overnight. Beads were added for 15 min then unbound beads were washed off. Cells were fixed with 3.7% paraformaldehyde and mounted on coverslips. Coverslips were then imaged using a 20x objective (Zeiss plan-Apochromat 20x/0.8) with a Zeiss axiovert 200 M microscope with a Hamamatsu ORCA-ERAG digital camera and MetaMorph software.

Immunoprecipitation

HUVECs were lysed on ice for 30 min in lysis buffer (10 mM Tris, pH 7.4, 150 mM NaCl, 1% Triton X-100, 0.5% NP-40, containing 1mM PMSF, and 10 μg/ml aprotinin and leupeptin, and 10 μg/ml orthovanadate). Lysates were precleared with protein A/G-agarose beads, and then incubated with LARG pAb overnight at 4 °C. A/G-agarose beads added for 1 h at 4 °C, then were sedimented and washed in lysis buffer at 4°C, resuspended in sample buffer, boiled for 10 min, and analyzed by Western blotting.

Viral shRNA Knockdown of protein expression

The targeted sequence for LARG was GCGAGTATCCAGAGAAGGAAT and prepared by the UNC lenti-shRNA core. ECs were grown to 80% confluency and infected with the lowest amount of viral particles to ensure sufficient knockdown (KD) at 48 h. Infected cells were then selected with 2.5 μg/ml puromycin for 24 h. For biochemical experiments, ECs were allowed to grow until confluent. For imaging experiments ECs were re-plated at confluence. RhoA knockdown re-expression was achieved using adenovirus miRNA and WT RhoA re-expression as previously described (35). After KD and RhoA rescue, cells were re-plated at a high density for experimental assays.

Electrical impedance measurement of monolayer integrity

After puromycin selection, high density HMVECs were plated on SIM plates (Roche Applied Science) coated with 6 μg/ml collagen. Electrical impedance was measured using the xCELLigence Real-Time Cell Analyzer (RTCA) system (Roche Applied Science). Each experiment was performed in triplicate and repeated 3 times.

Live-cell imaging

HMVECs were grown on collagen-coated glass dishes (MatTek Corporation) for at least 72 h before imaging. HMVECs were treated with 5 ng/ml TNF overnight. Neutrophils were added for 10 min then unbound cells were washed off. Cells were then imaged at 37°C and 5% CO_2 using a 20x objective (Zeiss plan-Apochromat 20x/0.8) with a Zeiss axiovert 200 M microscope with a Hamamatsu ORCA-ERAG digital camera and MetaMorph software for 30 min in EC growth medium. A manual tracking plug-in (http://rsbweb.nih.gov/ij/

plugins/track/track.html) for Image J software (NIH) was used to determine cell migration velocities.

TEM assay

TEM assays were performed in transwell plates (Corning, Corning, New York, U.S.) of 6.5-mm diameter with 8-μm pore filters. HMVECs were plated to generate a confluent monolayer on collagen-coated transwell filters and treated with 5 ng/ml TNF overnight. Neutrophils were added to the upper chamber and allowed to migrate across the monolayer to 25 ng/ml CXCL12 for 1 h at 37°C and 5% CO_2. The filters were fixed, stained with DAPI and neutrophils that had migrated to the lower chamber were counted by fluorescence microscopy using a 20x objective (Zeiss plan-Apochromat 20x/0.8) with a Zeiss axiovert 200 M microscope with a Hamamatsu ORCA-ERAG digital camera and MetaMorph software. The experiment was preformed four times in duplicate.

Statistical analysis

Statistical significance of data was determined using a two-tailed unpaired *t* test.

Results

Mechanical force on ICAM-1 increases cellular stiffness around ICAM-1 clusters

We first sought to determine if mechanical force on ICAM-1 induces a cellular response. We used beads coated with αICAM-1 mAb as a model to mimic leukocyte-induced ICAM-1 clustering (12). The beads were also magnetic, allowing us to apply force on the ICAM-1 clusters. To assess cellular stiffness, we measured displacement of attached beads during pulses of force (36–38). We applied pulses of 160 pN force on ICAM-1 and tracked the bead location during each pull (Fig. 1A). There was no statistically significant difference in the initial average displacements of the beads on cells grown on collagen (0.5 μm) or fibronectin (0.4 μm). We observed that after the first pulse of force subsequent pulses did not displace the beads as much, indicating cellular stiffening (Fig. 1B). This stiffening response occurred whether the ECs had been cultured on a fibronectin or collagen ECM, revealing that the response was not affected by the integrins through which the ECs were adhering to the matrix (Fig. 1B,C). Since there was little change in bead displacement between the second pulse and subsequent pulses, for most experiments we have compared the bead displacement generated by the first and second pulse.

To explore the basis for the force-induced stiffening, we examined the effects of agents that perturb the cytoskeleton. The average initial bead displacement for control cells, and cells treated with blebbistatin, cytochalasin D, Y-27632 and SU6656 were 0.4, 0.6, 0.8, 0.4, and 0.6 μm, respectively. The stiffening response was blocked by disrupting the actin cytoskeleton with cytochalasin D or by inhibiting myosin activity with blebbistatin (Fig. 1D). To inhibit the RhoA/ROCK pathway we used the ROCK inhibitor Y-27632 (Fig. 1D) and used adenoviral delivery of miRNA to KD RhoA expression (Fig. 1E, F). We found that KD of RhoA as well as inhibition of ROCK both inhibited the force-induced stiffening response. The SFK inhibitor, SU6656, also was able to prevent any change in bead displacement between pulses (Fig. 1D). Taken together these results suggest that ECs

respond to mechanical force on ICAM-1 and the observed stiffening response is dependent on the actin cytoskeleton, myosin activity, RhoA signaling and SFK activity.

RhoA is activated by mechanical force on ICAM-1

After we had determined that the cellular stiffening was dependent on RhoA expression and actomyosin contractility we next wanted to examine RhoA activity levels. A considerable body of work has revealed the importance of RhoA within ECs in facilitating the passage of leukocytes across the endothelium (4, 5, 14, 16). To cluster ICAM-1, we incubated cells for 15 min with magnetic beads coated with αICAM-1 mAb, and then applied force with a permanent magnet placed above the cell culture dish for 1 min to provide ~10 pN of force (Fig. 2A). Consistent with previous findings (3, 4, 16), ICAM-1 clustering increased RhoA activity over untreated cells (Fig. 2A). RhoA activity was further increased within 1 min of mechanical force on the ICAM-1 bead clusters (Fig. 2A). To evaluate if the observed activation of RhoA was specific to ICAM-1, we clustered and applied force on MHC class I. Neither clustering, nor force application on MHC class I significantly affected RhoA activity (Fig. 2B), confirming that the activation of RhoA is not a universal response to tension on the cell surface. Both MHC class I beads and the ICAM-1 mAb coated beads were able to bind to the EC monolayer as seen by phase contrast microscopy (Fig. 2C). MLC phosphorylation is frequently elevated downstream from RhoA activation and this was observed paralleling the increase in RhoA activity as ICAM-1 was clustered and then subjected to force (Fig. 2D).

ICAM-1 signaling activates LARG

While a downstream role for RhoA activity after ICAM-1 engagement has long been established, the GEF mediating activation of RhoA has not been determined. Using the binding of GEFs to nucleotide-free mutant $RhoA^{G17A}$ as an indicator of GEF activation (34), we tested several candidate GEFs including LARG, p190RhoGEF p115RhoGEF, GEF-H1 and PDZ-RhoGEF, but only observed activation of LARG in response to ICAM-1 clustering (Fig 3A–E). There was an additional increase in LARG activity when force was applied to the clustered ICAM-1 (Fig. 3A). Neither clustering MHC class I, nor applying tension on this receptor affected LARG activity (Fig. 3F). ICAM-1 clustering induced LARG tyrosine phosphorylation and application of force on ICAM-1 further elevated this phosphorylation (Fig. 3G). Treatment of cells with the SFK inhibitor, SU6656, inhibited LARG activation induced by ICAM-1 clustering and greatly attenuated LARG activation after ICAM-1 clustering with force (Fig. 3H). These results strongly suggest a pathway in which clustering of ICAM-1 activates SFKs (19, 26–28) to phosphorylate and activate LARG.

Knockdown of LARG expression inhibits RhoA activation downstream of ICAM-1 clustering

To further investigate whether LARG activation is responsible for the increase in RhoA activity downstream of ICAM-1 signaling, we used lenti-shRNA technology to depress LARG expression. ECs were infected with LARG shRNA or scrambled control shRNA. We confirmed by immunoblotting that LARG protein levels were reduced by the lenti-shRNA treatment and that the levels of similar GEFs like p115 were not decreased (Fig. 4A).

Interestingly, p115RhoGEF showed a slight increase in expression in response to LARG knockdown. TNF induction of ICAM-1 expression was preserved with control and LARG shRNA treatment (Fig. 4B). We also sought to confirm that LARG KD did not alter resting junctional permeability. This was examined by assaying electrical impedance (Fig. 4C). After LARG KD there was no RhoA activation in response to ICAM-1 clustering or when force was applied to the ICAM-1 clusters (Fig. 5A). The control shRNA-treated ECs exhibited ICAM-1-clustering and force-dependent RhoA activation similar to wild type ECs (Fig. 5B). To determine if LARG KD affected the cellular stiffness at ICAM-1 clusters, we used magnetic tweezers as in figure 1. We measured the stiffness of the cells with a single pulse of force on ICAM-1 (Fig. 5C). The stiffness measured was 50 Pa in control cells compared to 37 Pa in LARG KD cells. While there was a reproducible trend of ECs becoming softer after LARG KD, this difference was not statistically significant. However, after LARG KD there was a loss of the adaptive stiffening at ICAM-1 clusters in response to force after the first pulse. Compared to the control KD ECs or untreated cells, LARG KD ECs revealed no change in bead displacement between the first and second pulse (Fig. 5D).

To determine whether ICAM-1-induced stiffening might contribute to increased leukocyte migration over the EC surface, we disrupted this pathway by knocking down LARG expression. Neutrophils were plated on a TNF-treated EC monolayers and live cell imaging was used to calculate the average velocity of neutrophil migration. For neutrophils crawling on control KD ECs, the average velocity was 3 μm/min, whereas after LARG KD in ECs the average velocity decreased to 2.5 μm/min (Fig. 5E). Given that leukocytes migrate more rapidly over stiffer surfaces, these results are consistent with LARG-dependent stiffening of ECs induced by neutrophil traction enhancing neutrophil migration over the EC surface.

Endothelial LARG contributes to leukocyte TEM

To determine whether endothelial LARG contributes to neutrophil TEM, we counted and compared the number of neutrophils crossing a control shRNA EC monolayer with the number crossing a monolayer in which LARG expression had been decreased by shRNA. The percentage of leukocytes crossing the EC monolayer after LARG KD was decreased by ~35% compared with the control EC monolayer (Fig. 5F). These results show that LARG activity in ECs promotes both neutrophil migration over the endothelial surface as well as neutrophil TEM.

Discussion

Leukocyte TEM is an essential step in the recruitment of leukocytes out of the blood circulation and into tissues during inflammation. In order for TEM to occur, leukocytes must first adhere to the endothelium and this is mediated by receptors on both the leukocyte and ECs. ICAM-1 is a key endothelial receptor which functions as a ligand for β2 integrins on the surface of leukocytes, promoting leukocyte spreading and migration (39). However, ICAM-1 is more than an adhesive ligand, its engagement and clustering by the leukocyte generates many signals in ECs that promote TEM (15). It is widely considered that increased RhoA activity downstream from ICAM-1 clustering (5, 16) contributes to leukocyte TEM both by weakening the junctions and increasing tension on them to open them (4, 13, 15, 21,

40, 41). At the outset of this work, we were interested in identifying the GEF(s) responsible for RhoA activation downstream of ICAM-1, and secondly, we were interested in determining whether the tractional forces exerted on ICAM-1 as leukocytes migrate affect RhoA signaling. Here we identify LARG as the critical RhoA GEF activating RhoA downstream of ICAM-1, show that it is activated by SFK-dependent tyrosine phosphorylation, and demonstrate that applying mechanical force on ICAM-1 clusters equivalent to the forces generated by migrating neutrophils enhances this signaling pathway. This is the first report of RhoA activation downstream of ICAM-1 being regulated by SFKs. The stiffness of the ECs at ICAM-1 clusters is of great importance as this is where the leukocyte makes contact with the endothelial cell, exerts tractional force and senses the endothelial cell stiffness. We provide evidence that this activation of RhoA not only promotes neutrophil TEM but stiffens the endothelial surface which may enhance the migration of neutrophils over it.

Our first goal in this work was to identify the GEF(s) downstream from ICAM-1 responsible for activating RhoA. Several RhoA GEFs have been identified in signaling pathways initiated by other cell adhesion molecules. For example, in response to integrin-mediated adhesion on fibronectin, p115 RhoGEF and LARG were found in one study (32) and p190RhoGEF was implicated in another (42). Tension on fibronectin-based adhesions further activated RhoA through LARG and GEF-H1 (37). LARG has also been identified in association with CD44 (43), whereas p114RhoGEF and GEF-H1 have been associated with tight junctions (44, 45). Together with p115RhoGEF and PDZ-RhoGEF, LARG belongs to the RGS family of RhoA GEFs, implying that it can be activated downstream of G protein-coupled receptors via binding to Gα12/13. However, it can also be activated downstream from integrin engagement as well as following mechanical force on integrins (32, 37). In the latter case, activation of LARG was induced by tyrosine phosphorylation, either directly or indirectly by the SFK Fyn (37). Downstream from ICAM-1 clustering and tension on ICAM-1, we observed that LARG was activated and tyrosine phosphorylated in a time course that paralleled RhoA activation and that a SFK inhibitor blocked this response. SFKs not only have been shown to be activated downstream of ICAM-1 signaling (19, 27, 46) but LARG has also been shown to be a substrate of SFKs (37, 47). KD of LARG expression in ECs blocked ICAM-1-mediated activation of RhoA, confirming that LARG is critical for RhoA activation downstream of ICAM-1. We found that p115RhoGEF expression does increase after LARG KD. This increase in p115RhoGEF expression is not sufficient to restore RhoA activity downstream of ICAM-1, however it may well be that p115RhoGEF activity compensates for other signaling pathways in the LARG KD cells. Our results strongly suggest a pathway in which clustering of ICAM-1 activates SFKs that phosphorylate and activate LARG. Our results also indicate that mechanical tension on ICAM-1 clusters enhances this pathway leading to higher levels of LARG tyrosine phosphorylation, increased activation and elevated levels of GTP-loaded RhoA. These findings point to LARG as the major regulator of RhoA activity downstream of ICAM-1 signaling.

Previous studies examining endothelial compliance have obtained conflicting results in response to leukocyte adhesion. Initially, using magnetic twisting cytometry to pull on integrins, it was found that clustering of ICAM-1 or adhesion of neutrophils to ECs induced

a stiffening response (48, 49). This is of great interest as it is the region of the cell the leukocyte would be in contact with and sensing. In contrast, subsequent work by the same group using atomic force microscopy found transient and localized softening of the endothelial surface in a zone around where neutrophils adhered but an increased stiffening of adjacent cells (50). These differences likely result in part from the different techniques used to measure stiffness, but they may also reflect slight differences in culture conditions with the former favoring paracellular transmigration (i.e. passage through the junctions) and the latter favoring transcellular migration (i.e. passage through the EC body). Atomic force microscopy has also been used to show that treatments, such as TNF, or plating ECs on stiffer substrata, increase EC stiffness (51, 52). While there have been many studies looking at the role of EC behavior on substrata of different stiffness (52–56), here we observe that ECs alter the stiffness of their points of contact with leukocytes in response to tractional force generated by the leukocyte. The EC response we observe is independent of the type of ECM protein to which the ECs adhere. In the context of leukocyte migration, stiffer substrata have been linked to enhanced leukocyte crawling, adhesion and the generation of stronger tractional forces (30, 31, 57, 58). The finding that mechanical force on ICAM-1 induces a LARG-dependent endothelial stiffening provides a novel mechanism by which leukocytes can manipulate ECs to facilitate leukocyte TEM.

The recruitment of leukocytes from the blood circulation and into tissues is critical in the inflammatory response that contributes to defense of the host organism against invasion by infectious or other foreign agents. However, inappropriate recruitment and activation of leukocytes underlies many acute or chronic inflammatory diseases. In the search for new therapeutic targets to combat inflammatory diseases, strategies to inhibit leukocyte TEM continue to be investigated. Our finding here that inhibiting LARG in ECs decreases TEM, suggests that LARG may be a suitable anti-inflammatory target that is more specific than targeting RhoA activity itself which has diverse functions in many cells. Several studies have recently aimed at developing inhibitors of GEFs including LARG (59, 60), making this an exciting direction to pursue in the future.

Acknowledgments

We gratefully acknowledge Dr. Erika Wittchen for her experimental advice and critical reading of the manuscript. We thank Lisa Sharek for her technical support.

ECL was supported by NIH predoctoral training grant (T32 HL069768) and by a predoctoral fellowship from the American Heart Association (12PRE11780065). CG was supported by a Marie Curie Outgoing International Fellowship from the European Union Seventh Framework Programme (*FP7/2007-2013*) under grant agreement n° 254747. This work was supported by NIH grants HL080166, HL114388, GM029860 (KB) and P41-EB002025-23A1 (RS).

Abbreviations List

EC	endothelial cell
GEF	guanine nucleotide exchange factor
ICAM-1	inter-cellular adhesion molecule-1
HMVEC	human microvascular endothelial cells

KD	knockdown
MLC	myosin light chain
pMLC	phosphorylated myosin light chain
SFK	src family kinase
TEM	transendothelial cell migration

References

1. Butcher EC. Leukocyte-endothelial cell recognition: three (or more) steps to specificity and diversity. Cell. 1991; 67:1033–1036. [PubMed: 1760836]
2. Dustin ML, Springer TA. Lymphocyte function-associated antigen-1 (LFA-1) interaction with intercellular adhesion molecule-1 (ICAM-1) is one of at least three mechanisms for lymphocyte adhesion to cultured endothelial cells. J Cell Biol. 1988; 107:321–331. [PubMed: 3134364]
3. Wojciak-Stothard B, Williams L, Ridley AJ. Monocyte adhesion and spreading on human endothelial cells is dependent on Rho-regulated receptor clustering. J Cell Biol. 1999; 145:1293–1307. [PubMed: 10366600]
4. Adamson P, Etienne S, Couraud PO, Calder V, Greenwood J. Lymphocyte migration through brain endothelial cell monolayers involves signaling through endothelial ICAM-1 via a rho-dependent pathway. J Immunol. 1999; 162:2964–2973. [PubMed: 10072547]
5. Thompson PW, Randi AM, Ridley AJ. Intercellular adhesion molecule (ICAM)-1, but not ICAM-2, activates RhoA and stimulates c-fos and rhoA transcription in endothelial cells. J Immunol. 2002; 169:1007–1013. [PubMed: 12097408]
6. Carman CV, Jun CD, Salas A, Springer TA. Endothelial cells proactively form microvilli-like membrane projections upon intercellular adhesion molecule 1 engagement of leukocyte LFA-1. J Immunol. 2003; 171:6135–6144. [PubMed: 14634129]
7. Carman CV, Springer TA. A transmigratory cup in leukocyte diapedesis both through individual vascular endothelial cells and between them. J Cell Biol. 2004; 167:377–388. [PubMed: 15504916]
8. Yang L, Froio RM, Sciuto TE, Dvorak AM, Alon R, Luscinskas FW. ICAM-1 regulates neutrophil adhesion and transcellular migration of TNF-alpha-activated vascular endothelium under flow. Blood. 2005; 106:584–592. [PubMed: 15811956]
9. Carman CV, Sage PT, Sciuto TE, de la Fuente MA, Geha RS, Ochs HD, Dvorak HF, Dvorak AM, Springer TA. Transcellular diapedesis is initiated by invasive podosomes. Immunity. 2007; 26:784–797. [PubMed: 17570692]
10. Oh HM, Lee S, Na BR, Wee H, Kim SH, Choi SC, Lee KM, Jun CD. RKIKK motif in the intracellular domain is critical for spatial and dynamic organization of ICAM-1: functional implication for the leukocyte adhesion and transmigration. Mol Biol Cell. 2007; 18:2322–2335. [PubMed: 17429072]
11. Muller WA. Mechanisms of transendothelial migration of leukocytes. Circ Res. 2009; 105:223–230. [PubMed: 19644057]
12. van Buul JD, Allingham MJ, Samson T, Meller J, Boulter E, Garcia-Mata R, Burridge K. RhoG regulates endothelial apical cup assembly downstream from ICAM1 engagement and is involved in leukocyte trans-endothelial migration. J Cell Biol. 2007; 178:1279–1293. [PubMed: 17875742]
13. Sans E, Delachanal E, Duperray A. Analysis of the roles of ICAM-1 in neutrophil transmigration using a reconstituted mammalian cell expression model: implication of ICAM-1 cytoplasmic domain and Rho-dependent signaling pathway. J Immunol. 2001; 166:544–551. [PubMed: 11123335]
14. Lyck R, Reiss Y, Gerwin N, Greenwood J, Adamson P, Engelhardt B. T-cell interaction with ICAM-1/ICAM-2 double-deficient brain endothelium in vitro: the cytoplasmic tail of endothelial ICAM-1 is necessary for transendothelial migration of T cells. Blood. 2003; 102:3675–3683. [PubMed: 12893765]

15. Wittchen ES. Endothelial signaling in paracellular and transcellular leukocyte transmigration. Frontiers in bioscience: a journal and virtual library. 2009; 14:2522–2545.
16. Etienne S, Adamson P, Greenwood J, Strosberg AD, Cazaubon S, Couraud PO. ICAM-1 signaling pathways associated with Rho activation in microvascular brain endothelial cells. J Immunol. 1998; 161:5755–5761. [PubMed: 9820557]
17. Carpen O, Pallai P, Staunton DE, Springer TA. Association of intercellular adhesion molecule-1 (ICAM-1) with actin-containing cytoskeleton and alpha-actinin. J Cell Biol. 1992; 118:1223–1234. [PubMed: 1355095]
18. Barreiro O, Yanez-Mo M, Serrador JM, Montoya MC, Vicente-Manzanares M, Tejedor R, Furthmayr H, Sanchez-Madrid F. Dynamic interaction of VCAM-1 and ICAM-1 with moesin and ezrin in a novel endothelial docking structure for adherent leukocytes. J Cell Biol. 2002; 157:1233–1245. [PubMed: 12082081]
19. Tilghman RW, Hoover RL. The Src-cortactin pathway is required for clustering of E-selectin and ICAM-1 in endothelial cells. FASEB J. 2002; 16:1257–1259. [PubMed: 12060669]
20. Yang L, Kowalski JR, Yacono P, Bajmoczi M, Shaw SK, Froio RM, Golan DE, Thomas SM, Luscinskas FW. Endothelial cell cortactin coordinates intercellular adhesion molecule-1 clustering and actin cytoskeleton remodeling during polymorphonuclear leukocyte adhesion and transmigration. J Immunol. 2006; 177:6440–6449. [PubMed: 17056576]
21. Strey A, Janning A, Barth H, Gerke V. Endothelial Rho signaling is required for monocyte transendothelial migration. FEBS Lett. 2002; 517:261–266. [PubMed: 12062449]
22. Wojciak-Stothard B, Entwistle A, Garg R, Ridley AJ. Regulation of TNF-alpha-induced reorganization of the actin cytoskeleton and cell-cell junctions by Rho, Rac, and Cdc42 in human endothelial cells. J Cell Physiol. 1998; 176:150–165. [PubMed: 9618155]
23. Essler M, Hermann K, Amano M, Kaibuchi K, Heesemann J, Weber PC, Aepfelbacher M. Pasteurella multocida toxin increases endothelial permeability via Rho kinase and myosin light chain phosphatase. J Immunol. 1998; 161:5640–5646. [PubMed: 9820544]
24. Carbajal JM, Schaeffer RC Jr. RhoA inactivation enhances endothelial barrier function. Am J Physiol. 1999; 277:C955–964. [PubMed: 10564088]
25. Yamamoto M, Ramirez SH, Sato S, Kiyota T, Cerny RL, Kaibuchi K, Persidsky Y, Ikezu T. Phosphorylation of claudin-5 and occludin by rho kinase in brain endothelial cells. Am J Pathol. 2008; 172:521–533. [PubMed: 18187566]
26. Etienne-Manneville S, Manneville JB, Adamson P, Wilbourn B, Greenwood J, Couraud PO. ICAM-1-coupled cytoskeletal rearrangements and transendothelial lymphocyte migration involve intracellular calcium signaling in brain endothelial cell lines. J Immunol. 2000; 165:3375–3383. [PubMed: 10975856]
27. Wang Q, Pfeiffer GR 2nd, Gaarde WA. Activation of SRC tyrosine kinases in response to ICAM-1 ligation in pulmonary microvascular endothelial cells. J Biol Chem. 2003; 278:47731–47743. [PubMed: 14504278]
28. Yang L, Kowalski JR, Zhan X, Thomas SM, Luscinskas FW. Endothelial cell cortactin phosphorylation by Src contributes to polymorphonuclear leukocyte transmigration in vitro. Circ Res. 2006; 98:394–402. [PubMed: 16385081]
29. Guilford WH, Lantz RC, Gore RW. Locomotive forces produced by single leukocytes in vivo and in vitro. Am J Physiol. 1995; 268:C1308–1312. [PubMed: 7762625]
30. Smith LA, Aranda-Espinoza H, Haun JB, Dembo M, Hammer DA. Neutrophil traction stresses are concentrated in the uropod during migration. Biophys J. 2007; 92:L58–60. [PubMed: 17218464]
31. Rabodzey A, Alcaide P, Luscinskas FW, Ladoux B. Mechanical forces induced by the transendothelial migration of human neutrophils. Biophys J. 2008; 95:1428–1438. [PubMed: 18390614]
32. Dubash AD, Wennerberg K, Garcia-Mata R, Menold MM, Arthur WT, Burridge K. A novel role for Lsc/p115 RhoGEF and LARG in regulating RhoA activity downstream of adhesion to fibronectin. J Cell Sci. 2007; 120:3989–3998. [PubMed: 17971419]
33. Ren XD, Kiosses WB, Schwartz MA. Regulation of the small GTP-binding protein Rho by cell adhesion and the cytoskeleton. EMBO J. 1999; 18:578–585. [PubMed: 9927417]

34. Garcia-Mata R, Wennerberg K, Arthur WT, Noren NK, Ellerbroek SM, Burridge K. Analysis of activated GAPs and GEFs in cell lysates. Methods Enzymol. 2006; 406:425–437. [PubMed: 16472675]
35. Aghajanian A, Wittchen ES, Campbell SL, Burridge K. Direct activation of RhoA by reactive oxygen species requires a redox-sensitive motif. PloS one. 2009; 4:e8045. [PubMed: 19956681]
36. Matthews BD, Overby DR, Mannix R, Ingber DE. Cellular adaptation to mechanical stress: role of integrins, Rho, cytoskeletal tension and mechanosensitive ion channels. J Cell Sci. 2006; 119:508–518. [PubMed: 16443749]
37. Guilluy C, Swaminathan V, Garcia-Mata R, O'Brien ET, Superfine R, Burridge K. The Rho GEFs LARG and GEF-H1 regulate the mechanical response to force on integrins. Nat Cell Biol. 2011; 13:722–727. [PubMed: 21572419]
38. Collins C, Guilluy C, Welch C, O'Brien ET, Hahn K, Superfine R, Burridge K, Tzima E. Localized tensional forces on PECAM-1 elicit a global mechanotransduction response via the integrin-RhoA pathway. Curr Biol. 2012; 22:2087–2094. [PubMed: 23084990]
39. Marlin SD, Springer TA. Purified intercellular adhesion molecule-1 (ICAM-1) is a ligand for lymphocyte function-associated antigen 1 (LFA-1). Cell. 1987; 51:813–819. [PubMed: 3315233]
40. WojciakStothard B, Williams L, Ridley AJ. Monocyte adhesion and spreading on human endothelial cells is dependent on Rho-regulated receptor clustering. Journal of Cell Biology. 1999; 145:1293–1307. [PubMed: 10366600]
41. Aghajanian A, Wittchen ES, Allingham MJ, Garrett TA, Burridge K. Endothelial cell junctions and the regulation of vascular permeability and leukocyte transmigration. Journal of thrombosis and haemostasis: JTH. 2008; 6:1453–1460. [PubMed: 18647230]
42. Lim Y, Lim ST, Tomar A, Gardel M, Bernard-Trifilo JA, Chen XL, Uryu SA, Canete-Soler R, Zhai J, Lin H, Schlaepfer WW, Nalbant P, Bokoch G, Ilic D, Waterman-Storer C, Schlaepfer DD. PyK2 and FAK connections to p190Rho guanine nucleotide exchange factor regulate RhoA activity, focal adhesion formation, and cell motility. J Cell Biol. 2008; 180:187–203. [PubMed: 18195107]
43. Bourguignon LY, Gilad E, Brightman A, Diedrich F, Singleton P. Hyaluronan-CD44 interaction with leukemia-associated RhoGEF and epidermal growth factor receptor promotes Rho/Ras co-activation, phospholipase C epsilon-Ca2+ signaling, and cytoskeleton modification in head and neck squamous cell carcinoma cells. J Biol Chem. 2006; 281:14026–14040. [PubMed: 16565089]
44. Benais-Pont G, Punn A, Flores-Maldonado C, Eckert J, Raposo G, Fleming TP, Cereijido M, Balda MS, Matter K. Identification of a tight junction-associated guanine nucleotide exchange factor that activates Rho and regulates paracellular permeability. J Cell Biol. 2003; 160:729–740. [PubMed: 12604587]
45. Terry SJ, Zihni C, Elbediwy A, Vitiello E, Leefa Chong San IV, Balda MS, Matter K. Spatially restricted activation of RhoA signalling at epithelial junctions by p114RhoGEF drives junction formation and morphogenesis. Nat Cell Biol. 2011; 13:159–166. [PubMed: 21258369]
46. Allingham MJ, van Buul JD, Burridge K. ICAM-1-mediated, Src- and Pyk2-dependent vascular endothelial cadherin tyrosine phosphorylation is required for leukocyte transendothelial migration. J Immunol. 2007; 179:4053–4064. [PubMed: 17785844]
47. Chikumi H, Fukuhara S, Gutkind JS. Regulation of G protein-linked guanine nucleotide exchange factors for Rho, PDZ-RhoGEF, and LARG by tyrosine phosphorylation: evidence of a role for focal adhesion kinase. J Biol Chem. 2002; 277:12463–12473. [PubMed: 11799111]
48. Wang Q, Doerschuk CM. Neutrophil-induced changes in the biomechanical properties of endothelial cells: roles of ICAM-1 and reactive oxygen species. J Immunol. 2000; 164:6487–6494. [PubMed: 10843706]
49. Wang Q, Chiang ET, Lim M, Lai J, Rogers R, Janmey PA, Shepro D, Doerschuk CM. Changes in the biomechanical properties of neutrophils and endothelial cells during adhesion. Blood. 2001; 97:660–668. [PubMed: 11157482]
50. Kang I, Wang Q, Eppell SJ, Marchant RE, Doerschuk CM. Effect of neutrophil adhesion on the mechanical properties of lung microvascular endothelial cells. Am J Respir Cell Mol Biol. 2010; 43:591–598. [PubMed: 20023207]

51. Stroka KM, Vaitkus JA, Aranda-Espinoza H. Endothelial cells undergo morphological, biomechanical, and dynamic changes in response to tumor necrosis factor-alpha. European biophysics journal: EBJ. 2012; 41:939–947. [PubMed: 22940754]
52. Stroka KM, Aranda-Espinoza H. Endothelial cell substrate stiffness influences neutrophil transmigration via myosin light chain kinase-dependent cell contraction. Blood. 2011; 118:1632–1640. [PubMed: 21652678]
53. Huynh J, Nishimura N, Rana K, Peloquin JM, Califano JP, Montague CR, King MR, Schaffer CB, Reinhart-King CA. Age-related intimal stiffening enhances endothelial permeability and leukocyte transmigration. Science translational medicine. 2011; 3:112ra122.
54. Birukova AA, Tian X, Cokic I, Beckham Y, Gardel ML, Birukov KG. Endothelial barrier disruption and recovery is controlled by substrate stiffness. Microvascular research. 2013
55. Byfield FJ, Reen RK, Shentu TP, Levitan I, Gooch KJ. Endothelial actin and cell stiffness is modulated by substrate stiffness in 2D and 3D. Journal of biomechanics. 2009; 42:1114–1119. [PubMed: 19356760]
56. Krishnan R, Klumpers DD, Park CY, Rajendran K, Trepat X, van Bezu J, van Hinsbergh VW, Carman CV, Brain JD, Fredberg JJ, Butler JP, van Nieuw Amerongen GP. Substrate stiffening promotes endothelial monolayer disruption through enhanced physical forces. American journal of physiology Cell physiology. 2011; 300:C146–154. [PubMed: 20861463]
57. Jannat RA, Robbins GP, Ricart BG, Dembo M, Hammer DA. Neutrophil adhesion and chemotaxis depend on substrate mechanics. Journal of physics Condensed matter: an Institute of Physics journal. 2010; 22:194117. [PubMed: 20473350]
58. Jannat RA, Dembo M, Hammer DA. Traction forces of neutrophils migrating on compliant substrates. Biophys J. 2011; 101:575–584. [PubMed: 21806925]
59. Evelyn CR, Ferng T, Rojas RJ, Larsen MJ, Sondek J, Neubig RR. High-throughput screening for small-molecule inhibitors of LARG-stimulated RhoA nucleotide binding via a novel fluorescence polarization assay. J Biomol Screen. 2009; 14:161–172. [PubMed: 19196702]
60. Shang X, Marchioni F, Evelyn CR, Sipes N, Zhou X, Seibel W, Wortman M, Zheng Y. Small-molecule inhibitors targeting G-protein-coupled Rho guanine nucleotide exchange factors. Proc Natl Acad Sci U S A. 2013; 110:3155–3160. [PubMed: 23382194]

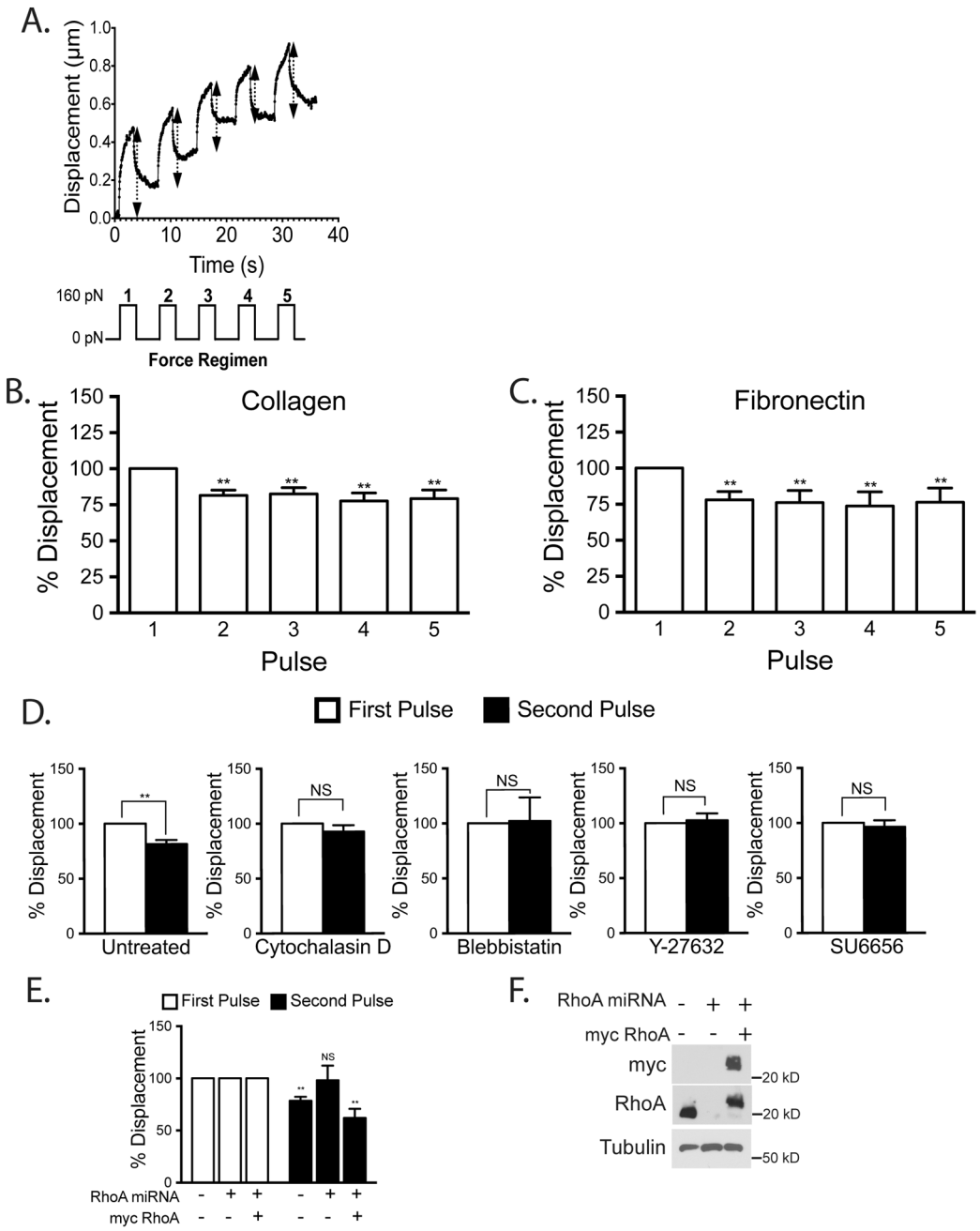

Figure 1.

Mechanical force on ICAM-1 increases cellular stiffening. Magnetic beads coated with ICAM-1 mAb were added to a monolayer of TNF-treated HMVECs. Magnetic tweezers were used to apply pulses of force to individual beads and bead movement recorded with high-speed video. (A) Typical displacement of a bead bound to ICAM-1. Arrows denote displacement distance (Top). A diagram of the 160 pN force regimen used (3s of force with 5s recovery for 5 pulses) (Lower). Percentage bead displacement in response to sequential pulses of force for ECs plated on collagen (B) or fibronectin (C). For D–F, the ECs were plated on collagen. (D) Bead displacements on HMVECs treated with specified inhibitors

for 30 min followed by 2 pulses of force. (E) Bead displacement on HMVECs and HMVECs treated with miRNA to inhibit RhoA expression with or without rescue with myc-RhoA. (F) Western blotting confirms RhoA KD and myc-RhoA re-expression. (B–E) Quantification of bead displacement with each pulse normalized to the first pulse. Asterisks shows *p*-value of statistical significance compared to the control (*, $p \leq 0.05$; **, $p \leq 0.01$). The means ± SEM of ≥9 independent bead pulls are shown.

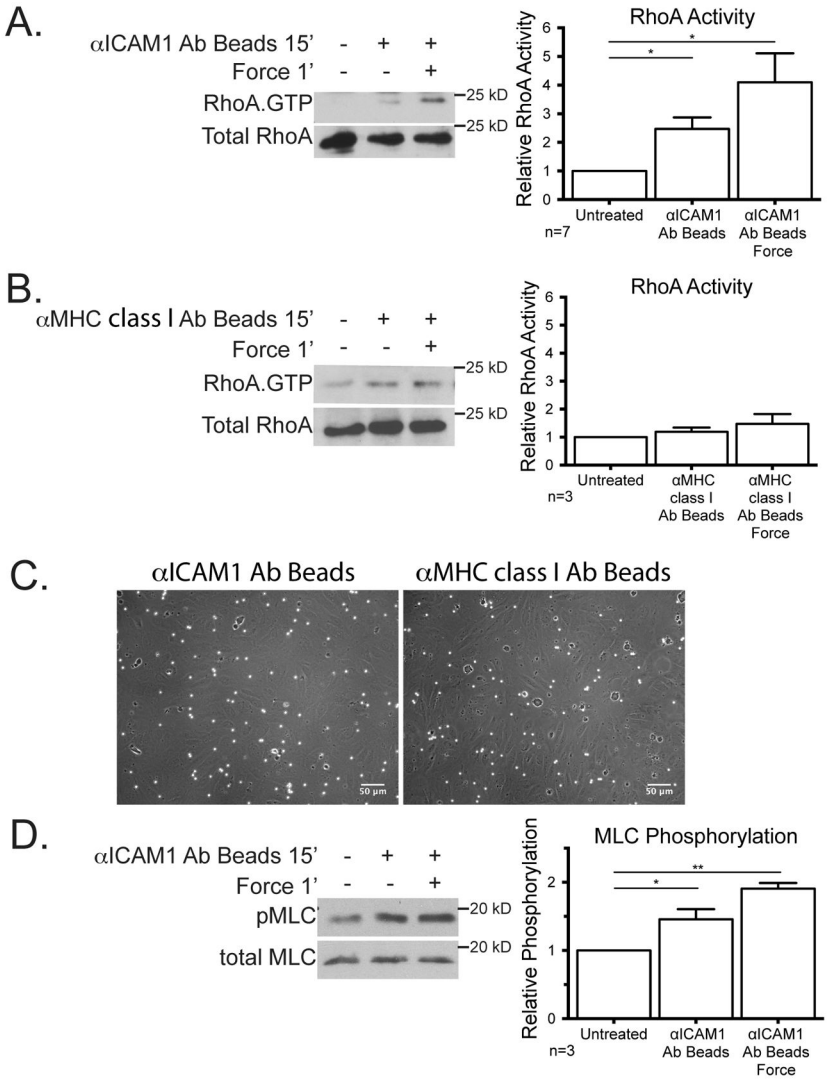

Figure 2.

Mechanical force on ICAM-1 increases RhoA activity and MLC phosphorylation. Magnetic beads coated with mAb against ICAM-1 (A, C, and D) or MHC class I (B and C) were added for 15 min to a monolayer of TNF-treated HUVECs and ~10 pN force was applied with a ceramic magnet placed above the cells for 1 min. (A and B) Using GST-RBD, RhoA. GTP was isolated and detected by immunoblotting. (C) Phase contrast images of EC monolayers 15′ after beads were added and washed 2x with media before fixing. (D) Lysates were immunoblotted for total MLC or MLC phosphorylated on Thr18/Ser19. Graphs show quantification of RhoA activity (A and B) or pMLC levels (D) from ≥3 independent experiments. Graphs show the means ± SEM. Asterisk shows *p*-value of statistical significance compared to control (*, $p \leq 0.05$; **, $p \leq 0.01$).

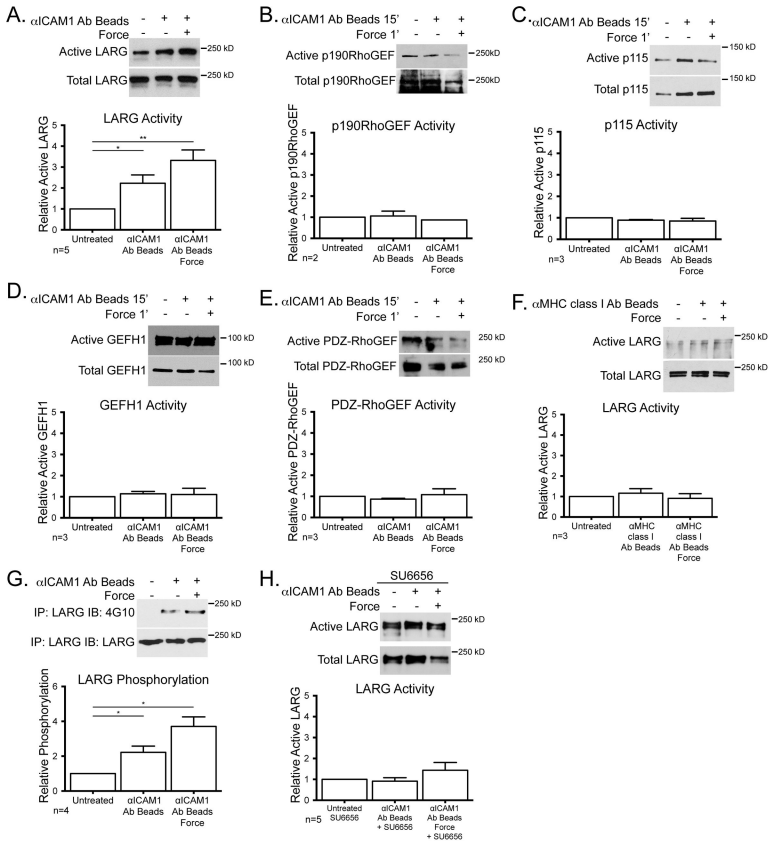

Figure 3.

LARG is activated downstream of ICAM-1 clustering alone and enhanced with mechanical force. TNF-treated HUVECs were treated with mAb-coated beads. (A–F) GEF activity was determined by affinity purification via GST-RhoA^{G17A} and detected by immunoblotting for the specified GEF, LARG (A and F), p190RhoGEF (B), p115 (C), GEFH-1 (D), PDZ-RhoGEF (E). (G) LARG was immunoprecipitated and immunoblotted for phosphotyrosine and LARG. (H) Active LARG was detected by sedimentation with GST-RhoA^{G17A} in the presence of SU6656. For all experiments, a representative blot of ≥2 independent experiments is shown. Graphs show the means ± SEM. Asterisk shows *p*-value of statistical significance compared to control by *t* test (*, p≤0.05; **, p≤0.01).

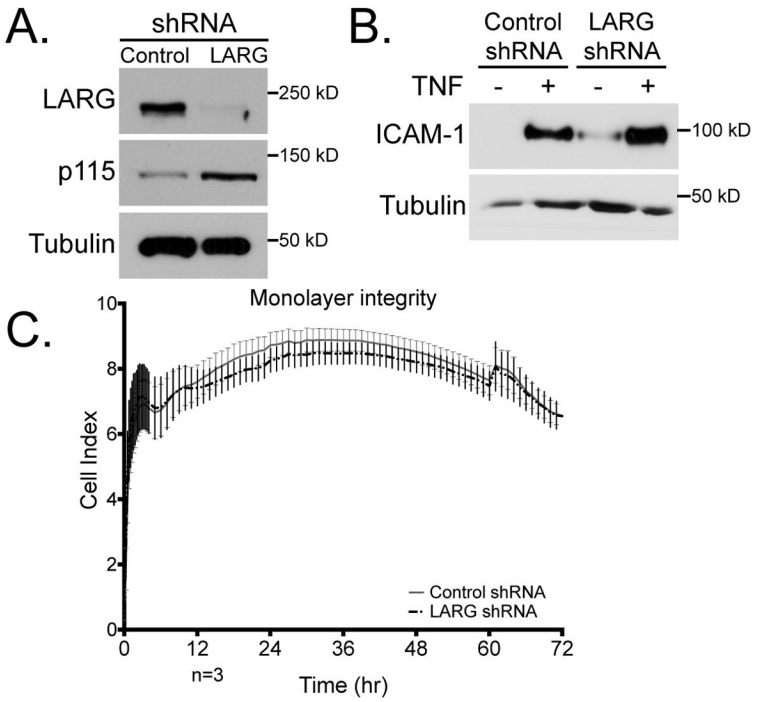

Figure 4.

Confirmation of LARG KD. HMVECs were treated with control or LARG shRNA lentivirus for 48 h and selected for with 2.5 ng/ml puromycin for 24 h. (A) EC lysates were immunoblotted with the indicated pAb. (B) Western blotting shows that ICAM-1 expression before and after TNF-treatment is not affected by LARG KD. (C) Electrical impedance was used to measure monolayer integrity for HMVECs plated at high density for 72 h. No significant difference was found in impedance values after control or LARG KD. *n*=3 independent experiments preformed in triplicate wells.

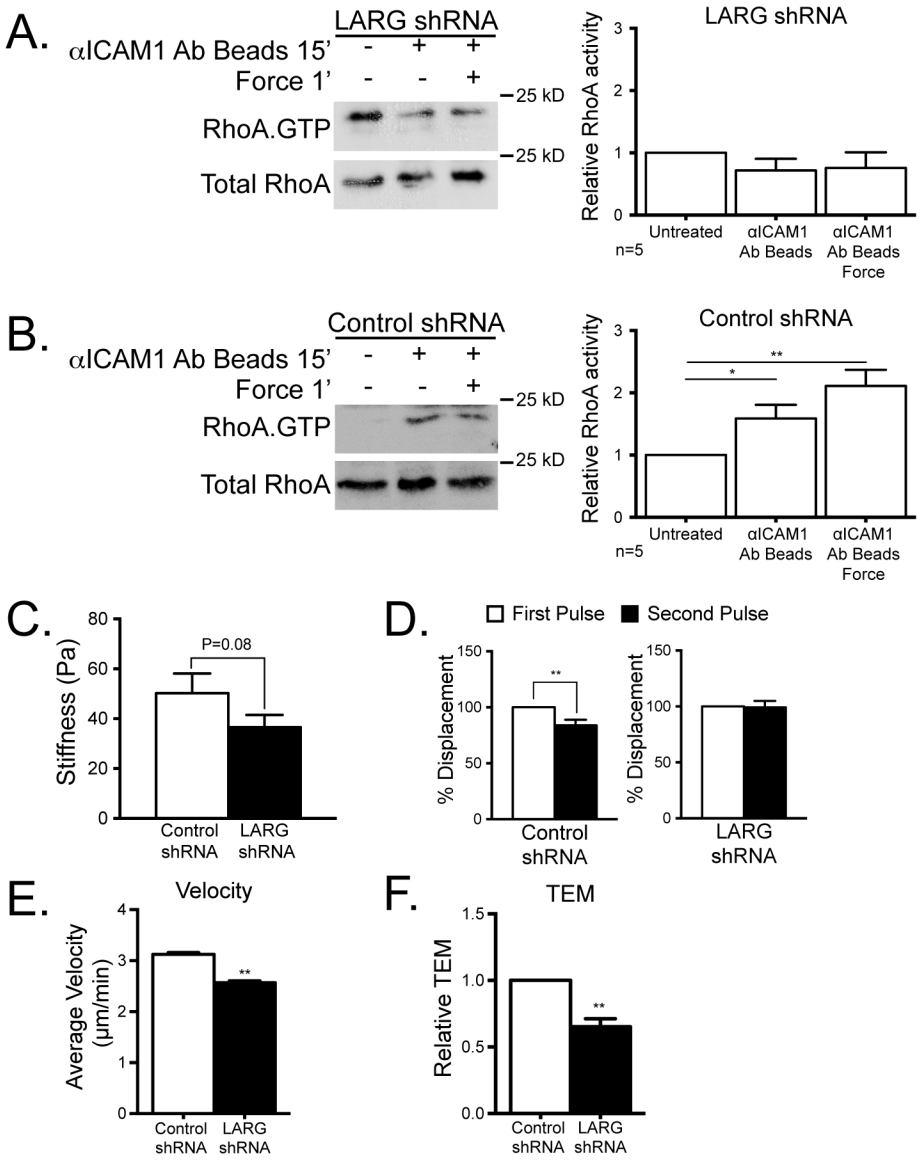

Figure 5.

LARG mediates EC response to mechanical force on ICAM-1 and affects neutrophil crawling and TEM. HUVECs were treated with control (B and C) or LARG (A and C) shRNA lenti-virus for 48 h and selected with 2.5 ng/ml puromycin for 24 h, then TNF-treated overnight. (A and B) RhoA activity was determined by immunoblotting after ICAM-1 clustering with or without force in HUVECs (left) and quantified (right). The means ± SEM of ≥4 independent experiments are shown. Asterisk shows *p*-value of statistical significance by *t* test (*, $p \leq 0.05$). (C) The stiffness of HMVECs was measured using magnetic tweezers and magnetic beads coated with ICAM-1 mAb. (D) Relative displacement of magnetic beads coated with ICAM-1 mAbs was measured in control HMVECs or in HMVECs in which LARG expression had been knocked down. The means ± SEM of N≥15 independent bead pulls are shown. Asterisk shows *p*-value of statistical significance by *t* test ($p \leq 0.01$). (E and F) Neutrophils were added to a monolayer of TNF-

treated HMVECs after LARG expression had been knocked down. (E) Neutrophils were imaged as they migrated over the HMVEC monolayer surface and their velocity was measured using tracking software. Data are the average of 3 experiments with ≥15 neutrophils measured per experiment. (F) The passage of neutrophils across a confluent EC monolayer was measured using transwell tissue culture inserts. Data are the average of 3 experiments each performed in duplicate. The means ± SEM are graphed. Asterisk shows *p*-value of statistical significance (*, $p \leq 0.05$; **, $p \leq 0.01$).